CMLS, Cell. Mol. Life Sci. 55 (1999) 1416–1431
1420-682X/99/111416-16 $ 1.50 + 0.20/0

CMLS Cellular and Molecular Life Sciences

Review

Intermediate filament assembly: temperature sensitivity and polymorphism

H. Herrmann[a,*] and U. Aebi[b]

[a]Division for Cell Biology, German Cancer Research Centre, D-69120 Heidelberg (Germany),
Fax + 49 6221 42 3404, e-mail: H.Herrmann@DKFZ-Heidelberg.de
[b]Biozentrum, M. E. Müller Institute for Structural Biology, University of Basel, CH-4056 Basel (Switzerland)

The authors dedicate this paper to the memory of their friend and coworker Markus Häner (deceased 12 June 1999)

Received 22 February 1999; received after revision 28 April 1999; accepted 28 April 1999

Abstract. Intermediate filament (IF) proteins are encoded by a large multigene family and form polymers with a uniform diameter of approximately 10 nm. However, although the cytoplasmic representatives all confirm to a unit-type structural principle leading to the formation of extended coiled coils, it is becoming increasingly clear that subunit arrangements and physical properties vary among the different filaments. Thus, the intricate tissue-specific expression pattern of individual IF proteins (especially, their co-expression with other members of the IF protein family or with IF-associated proteins to form obligatory heteropolymers) points to distinct functions acquired during evolution relevant to cellular homeostasis in various tissues.

Key words. Intermediate filaments; assembly; polymorphism; fibrous proteins; scanning transmission electron microscopy (STEM) temperature sensitivity.

The filament systems of eukaryotic cells

Actin and tubulin, globular proteins of known atomic structure [1–3], constitute the molecular building blocks of microfilaments (MFs) and microtubules (MTs) in the cytoplasm of all eukaryotic cells. These cytoskeletal filaments possess apparent diameters of 6–8 nm and 20–25 nm, respectively, and are 'closed' assemblies in terms of their lateral subunit interactions (i.e., those specifying the diameter of the filament). In contrast, intermediate filament (IF) proteins, so named because their filaments exhibit an apparent diameter (i.e., 8–12 nm) between that of MFs and MTs, fold into polypeptides with extended α-helical coiled coils similar to other fibrous proteins such as myosin, tropomyosin, or collagen [for reviews see refs 4–10]. As a consequence, these elongated, two-stranded α-helical coiled-coil molecules interact laterally and longitudinally at multiple sites, thereby yielding polymorphic 'open' supramolecular assemblies with the potential for lateral subunit addition and/or exchange [see ref. 11].

Although MTs and MFs are evolutionarily older than IFs (i.e., the latter have not been found in plants, fungi, or protists), it has become clear that IFs must have developed very early in eukaryotic evolution, in parallel with the emergence of animals, since (i) nearly all higher eukaryotic cells contain nuclear IFs [i.e., lamins; cf. ref. 12], and (ii) annelids, nematodes, and mollusks exhibit complex patterns of IF protein expression [7, 13]. To mention a very recent relevant finding, 'primitive' inver-

* Corresponding author.

tebrate chordates, such as the tunicate *Styela*, synthesize an IF protein in their muscle cells that is highly homologous to the mammalian muscle-specific IF protein desmin, including sequence identity at both ends of its α-helical rod, sequence motifs which are highly conserved throughout the entire IF protein superfamily [14]. Moreover, in the hypervariable amino-terminal end domain, this tunicate protein contains a sequence motif conserved in several IF proteins from frog to rat [15] and directly involved in filament assembly [16–19]. The more than 200 IF protein sequences known to date have revealed a structural design that is common to and characterizes all members of the IF multigene family: highly variable non-α-helical amino- and carboxy-terminal end domains flank a central rod domain consisting of distinct α-helical segments of conserved amino acid number and sequence, thus forming coil 1A, coil 1B, and coil 2 [8]. Within these three distinct α-helical segments there is a heptad repeat pattern with hydrophobic amino acids in positions 1 and 4, which causes IF proteins to form stable parallel two-stranded α-helical coiled coils via their central rod domain. These dimeric molecules can withstand denaturing conditions as strong as 6–8 M urea [20].

The eukaryotic cell has evolved a strict dependence on tubulin and actin: mitosis and cellular morphogenesis depend on MTs, while cytokinesis, as well as other myosin-powered movements, requires MFs. Thus, actin and tubulin polymers probably fulfilled essential functions at the level of the individual cell long before they became engaged by evolution in building complex cellular entities such as flagella, microvilli, axons, or sarcomeres. Moreover, one may assume that these proteins evolved to function efficiently at the optimal temperature of the particular organism. For those poikilotherm species that have to tolerate large temperature differences, these proteins must perform well over a wide range of temperature changes. Indeed, some members of the aquatic vertebrata (e.g., fishes) may live either at freezing temperatures or close to 50 °C [21]. Consequently, actin and tubulin are highly conserved with regard to their amino acid sequences, i.e., as housekeeping proteins that are of central importance for the eukaryotic cell.

Beginning with this basic cytoarchitectural framework, differentiating cells that aggregate into morphologically and functionally distinct tissues developed a third filament system possessing new structural and mechanical properties tailored to the needs of a multicellular organism, the IF system [22]. These proteins originally evolved to form part of the nuclear lamina, disassembling during mitosis, and were only later remodelled to serve cytoplasmic needs. Thus, cytoplasmic IFs do not contain a classical nuclear localization signal, residing in the non-helical carboxy-terminal domain of lamins, and all cytoplasmic IFs, with the exception of those expressed in invertebrates, have lost a 42-amino-acid sequence stretch from the first half of the central helical rod, which reduces the length of the affected helix 1B by roughly 6 nm [4, 7, 11, 12, 61]. IFs are highly viscoelastic under various conditions, in contrast to the other two cytoskeletal filament systems, and their resistance to deformation changes dramatically when they are mechanically stressed; i.e., under such conditions, IFs acquire a new mechanical property which has been called 'strain hardening' [23]. Thus, IF systems are not only able to resist high strains, but the more they are strained, the more resistant they become to further deformation, i.e., in response to being strained, their stiffness increases dramatically—hardening. These properties may enable intermediate filaments to play a central role in cellular response to mechanical forces.

Thermosensitivity of IF proteins

Mammalian MTs are strongly temperature sensitive and disassemble in vitro when cooled to 4 °C [24]. In contrast, IFs withstand the combined challenge of nonionic detergents, high salt concentration, ice-cold temperature, and homogenization. Indeed, IFs can be purified away from most other cytoskeletal proteins by repeatedly being subjected to harsh conditions that dissolve even MFs [25]. In vivo, however, IF meshworks may be strongly affected by temperature changes. For example, Schliwa and Euteneuer [26] demonstrated that the tonofilament system (i.e., the cytokeratin IFs) of warm-water teleost fish epidermal cells undergo a dramatic, yet reversible rearrangement when the cells are cooled to near 0 °C. Upon rewarming, these entangled filament masses reorganize back into extended IF meshworks within minutes. Similar structural transitions of cytokeratin IFs have been observed during embryogenesis of some amphibia [27]. These structural transitions are reminiscent of the reorganization of IFs during mitosis [28, 29]. Since such temperature-mediated IF changes have never been observed in vitro, it was concluded that they were not intrinsic to IFs but, rather, are caused by cellular factors, such as those involved in the spreading of IF networks, and possibly MTs.

The first evidence for the intrinsic thermosensitivity of an IF protein in the physiological temperature range came from work with amphibian vimentin. After cDNA transfection of *Xenopus laevis* vimentin into the vimentin-free bovine mammary gland epithelial cell line BMGE + H grown at 37 °C, it was observed that in most cells, IF arrays did not form, although occasional individual cells with more filamentous than aggregate-type staining were observed [17]. Moreover, with a mutant *Xenopus* vimentin missing the non-helical car-

boxy-terminal tail domain and thereby assembling considerably better than wild-type vimentin at room temperature (as determined by viscometric assays), short but apparently normal IFs were occasionally detected by immuno-electron microscopy in transfected BMGE + H cells grown at 37 °C. However, the majority of the immunopositive material was organized in aggregates exhibiting a periodic transverse banding pattern [30]. This observation, in turn, indicated that the frog protein was able to form IFs in mammalian cells, although filament assembly was at variance with some of the structural features of the frog vimentin at this temperature. Since frogs are normally reared at room temperature, the in vitro assembly properties of *Xenopus* vimentin were determined over a wide range of temperatures, and the optimum temperature was found to be around 28 °C [31]. At 37 °C under otherwise standard assembly conditions, however, *Xenopus* vimentin assembled into non-IF-type fibers of irregular diameter and rather short length (see fig. 1A, B). The non-IF nature of the fibrils formed at 37 °C was particularly evident in ultrathin-sectioned pellets obtained from centrifuged polymerized material. In contrast to uniform, filamentous structures seen at room temperature, the fibers formed at 37 °C revealed 20- to 40-nm granules often extending into irregularly contoured filaments (5–20 nm diameter) with a hairy coat (fig. 1C, D) [31].

In agreement with these in vitro observations, *Xenopus* vimentin formed extensive IF arrays in vivo when the stably transfected mammalian cells were transferred to 28 °C [31]. In particular, IFs appeared to grow out of non-filamentous, aggregated masses within a few hours, indicating that the protein, while trapped in a non-IF state, was actively reorganized upon shift to the permissive temperature. Indeed, vimentin assembled in the test tube at the 'non-productive' temperature (i.e., non-permissive for regular IF assembly) is able to reorganize, at least in part, to more IF-like fibers if shifted to the permissive temperature within half an hour after initiation of assembly. This was documented by viscometric experiments performed at 37 °C for increasing time periods followed by a shift to 23 °C. Accordingly, assembly can be carried out for up to 30 min at 37 °C, producing little viscosity increase during this incubation period, followed by a significant viscosity increase after shift to 23 °C (fig. 2) [31]. As observed by electron microscopy, after 5 min of assembly at 37 °C, *Xenopus* vimentin had formed predominantly globular aggregates of approximately 50–60 nm diameter (fig. 3A).

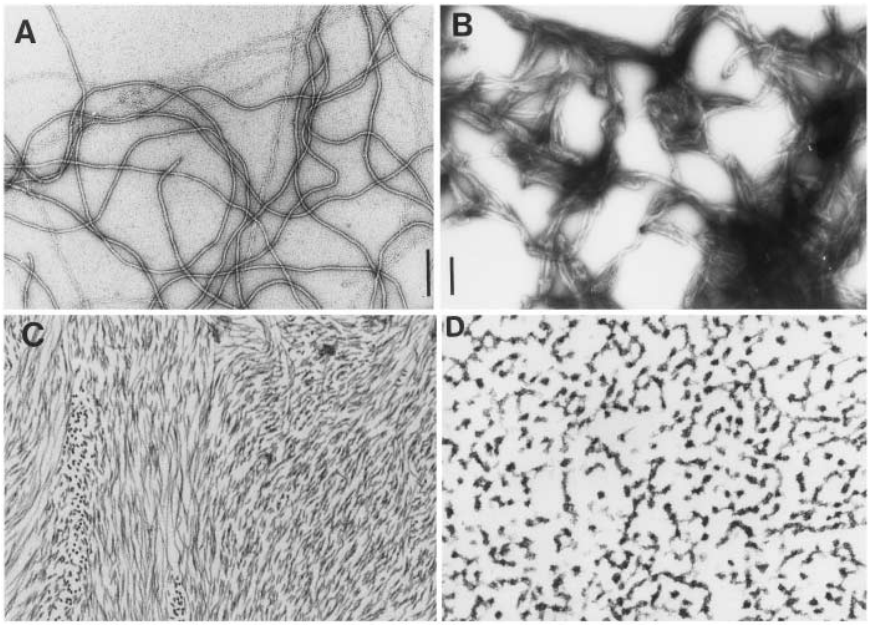

Figure 1. Temperature sensitivity of *Xenopus laevis* vimentin. Assembly was performed under standard conditions [see ref. 20] at room temperature (*A*, *C*) or 37 °C (*B*, *D*) for 1 h. Polymers formed were fixed and negatively stained (*A*, *B*) or pelleted in an Airfuge and processed for embedding and ultrathin sectioning (*C*, *D*). Note that at 37 °C, *Xenopus* vimentin forms rather heterogenous structures, i.e., short fibrils with diameters between 10 and 40 nm that often aggregate laterally with one another [for details see ref. 31]. Bars, 100 nm. Magnification in (*C*, *D*) is the same as in (*A*).

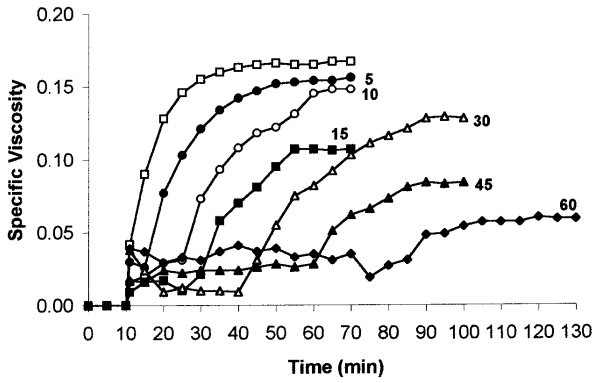

Figure 2. Viscosity measurements of recombinant *Xenopus* vimentin assembled for various times (5–60 min, as indicated to the right of the curves) at 37 °C, before being shifted to room temperature for the remaining time. Initiation of assembly was at 10 min; open squares show a control incubation performed at room temperature throughout [for details see ref. 31].

Similarly, after 5 h at 37 °C, the bulk of assembled material consisted of globular aggregates (fig. 3B). In contrast, when *Xenopus* vimentin, after 5 min of assembly at 37 °C, was transferred to 23 °C for another 30 min, practically no aggregates were encountered. Instead, only long filaments were seen that were occasionally irregularly thickened or even fused with a neighboring filament (arrows in fig. 3C).

Above its optimal assembly temperature (i.e., 28 °C in the case of *Xenopus* vimentin), normal IF formation becomes severely compromised even with a temperature rise of only 3 °C. Although the viscosity profiles obtained at 31 °C and 23 °C are similar [i.e., reaching about half the maximum value of the specific viscosity obtained at 28 °C; see ref. 31], the appearance in the electron microscope is completely different at the two suboptimal temperatures. IFs at 23 °C appear practically indistinguishable from those formed at 28 °C (fig. 3D). However, at 31 °C, predominantly long and rather 'spongy' (i.e., partially unravelled) filaments are observed even after 5 min (fig. 3E), which evidently fail to compact during the following 3-h incubation period at this temperature (fig. 3F). Nevertheless, a small number of more compact IFs with an apparent diameter ranging between 10 and 16 nm are present both at 5 min and 3 h. Similar to the situation at 37 °C, the compact filaments are often capped by globular aggregates (arrows in fig. 3F), which occur significantly less frequently in free form than at 37 °C (arrowheads in fig. 3E, F).

Taken together, these findings suggested that IF assembly, at least of *Xenopus* vimentin, is strikingly temperature sensitive. Therefore, the majority of the tetrameric complexes apparently assume a configuration that is incompatible with proper unit-length filament (ULF) assembly. Remarkably, the unassembled ULF-type aggregates (i.e., the distinct globular aggregates) are 'active,' in the sense that they are capable of terminating filament elongation (see fig. 3F). A more speculative, yet plausible view suggests that although attenuated, they can still take part in filament assembly by being structurally 'instructed' to rearrange before stably integrating into a bona fide IF.

At this point it was of interest to investigate whether IF proteins, in their fully folded soluble state, are heat stable, i.e., whether they withstand heating to high temperature (such as 80 °C) for extended times, yet remain competent for IF formation (Herrmann et al., unpublished data). As documented in figure 4, this was indeed the case for *Xenopus* vimentin, and it was also true for zebrafish, trout, and human vimentin (data not shown). Hence, one may conclude that the coiled-coil dimer (or the tetramer) stayed properly folded or regained, after cooling to 23 °C, the conformation required for assembly into bona fide IFs.

In contrast, at low temperature such as 4 °C, *Xenopus* vimentin forms long filaments which infrequently reveal 'partially unravelled' segments (fig. 5A, arrow) or exhibit distinct bead-like densities (fig. 5A, arrowheads). The partially unravelled filaments appeared to consist of protofibrils wound around each other in a right-handed fashion (fig. 5B) [see also ref. 32]. Similarly, human vimentin is also sensitive to cold: at 4 °C mainly unravelled filaments are observed. This is in contrast to vimentin from trout and zebrafish. Trout vimentin, which exhibits its temperature optimum for assembly at 18–24 °C, forms normal-looking IFs at low temperatures (4–12 °C), while producing mostly polymorphic, unravelled, or very thick irregular non-IF structures at 28 °C [33, 34]. Zebrafish vimentin, on the other hand, with an assembly optimum at 28 °C, yields considerable viscosity at 12 °C by producing long and unusually thick laterally interacting filaments [35]. At 15–18 °C, even thicker filaments, laterally aggregating over considerable distances, are produced. At 21 °C, however, apparently normal IFs form.

In summary, vimentin from different species, despite considerable sequence identity [33, 35], yields quite distinct filaments at a given temperature. Virtually indistinguishable, partially unravelled IFs are generated by trout vimentin at 28 °C, by *Xenopus* vimentin at 4 °C and 31 °C, and by human vimentin at 4 °C and 45 °C (unpublished data). In contrast, unusually thick filaments are produced by zebrafish vimentin between 12 °C and 18 °C, by trout vimentin after extended incubation at 28 °C [34], and by *Xenopus* vimentin at 37 °C [31]. These different types of filaments are, no doubt, formed by variations in dimer-dimer interactions and are composed of different numbers of subunits per

filament cross-section, thereby reflecting the structural versatility of these fibrous proteins.

Last but not least, temperature sensitivity of an IF system in vivo as a consequence of inherited point mutations in cytokeratins CK5 or CK14 has indeed been demonstrated in keratinocyte lines derived from patients with epidermolysis bullosa simplex [36]. Although under standard growth conditions the cytokeratin system did not exhibit any obvious abnormalities, upon thermal stress (i.e., raising the temperature for 15 min to 43 °C), the filaments were observed fragmenting into small aggregates. This phenotype is nearly completely reversed after 1 h of recovery from thermal stress. These experiments clearly demonstrate that IF structure (in this case with point mutations) is sensitive to temperature.

Amino acid sequence divergence of vimentins and desmins

A clue to those amino acids responsible for this distinct assembly behavior may be obtained by sequence comparison of vimentin from cold-water and warm-water fish, *X. laevis* and human. In general, the elementary building block of all IFs, the central α-helical rod domain, is about 80% identical between zebrafish, trout, *X. laevis* and human vimentin [33, 35]. On closer inspection, however, certain residues are unique to a particular species, the other three species being identical and different from the unique residue at these positions. For example, human vimentin has nine residues that differ from the other three species (fig. 6), whereas zebrafish

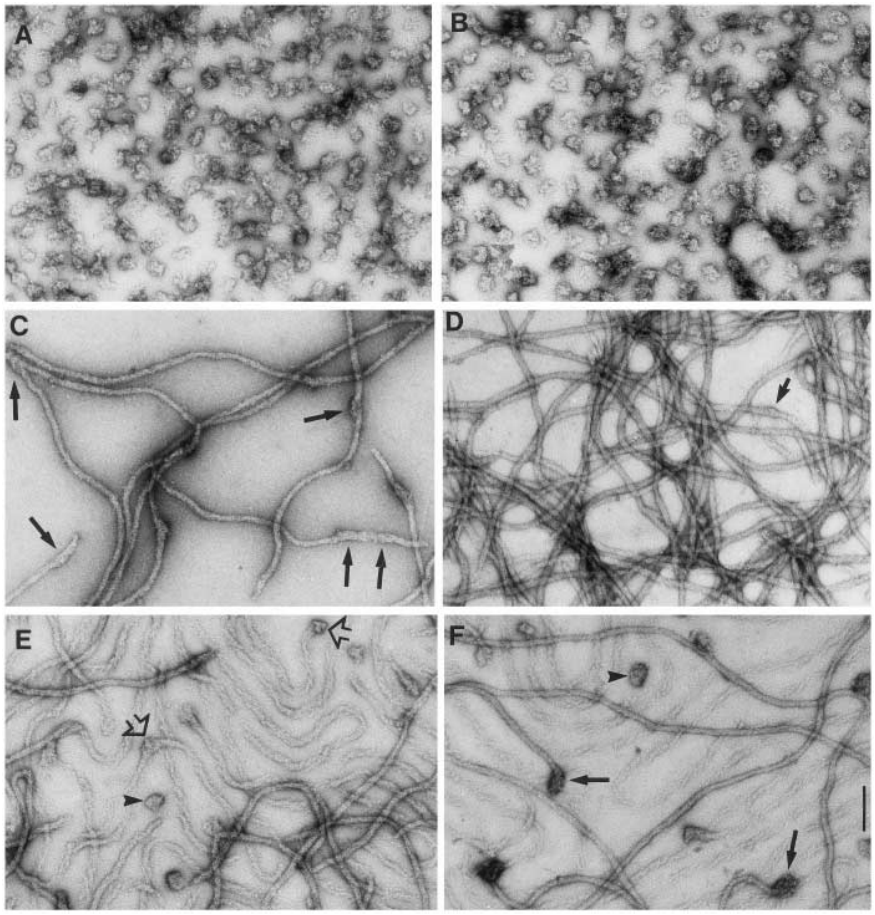

Figure 3. Electron microscopic analysis of negatively stained structures formed by *X. laevis* vimentin assembled at different temperatures and for different times: 5 min at 37 °C (*A*); 5 h at 37 °C (*B*); 5 min at 37 °C, before 30 min at 22 °C (*C*); 30 min at 22 °C (*D*); 5 min at 31 °C (*E*); 3 h at 31 °C (*F*). Assembly of soluble vimentin (in 5 mM Tris-HCl, pH 8.4) was initiated by addition of an equal volume of 'filament buffer' (45 mM Tris-HCl, pH 7.0, 100 mM NaCl), except for (*B*) which was performed by dialyzing the protein into a buffer of 25 mM Tris-HCl, pH 7.5, 50 mM NaCl. Arrowheads point to globular aggregates, possibly corresponding to unit-length-filament-type structures as formed at optimal assembly temperatures. Arrows mark apparent fusion events between temperature-induced aggregates and IFs. In (*E*) the open arrows denote fusion of aggregates with 'open' IFs. Bar, 100 nm.

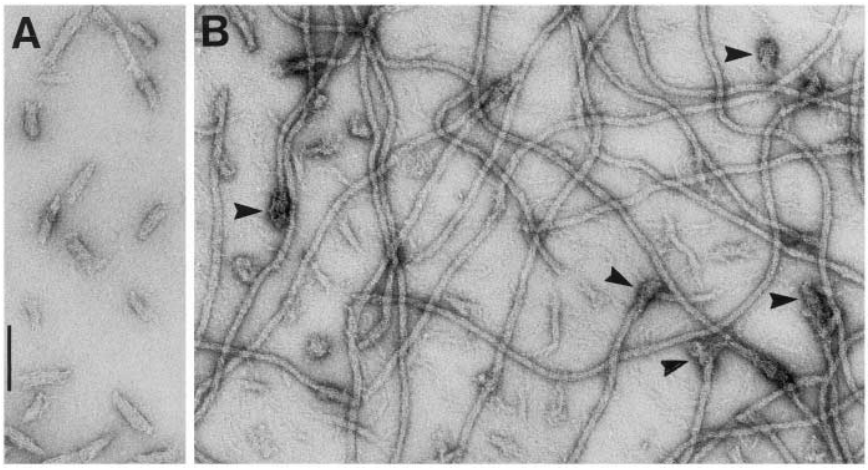

Figure 4. Heat stability of tetrameric vimentin. After heating for 10 min at 80 °C, *X. laevis* vimentin readily assembles into bona fide IFs upon cooling to room temperature, although some globular aggregates (as typically seen at 37 °C) are also present. Note that most of these aggregates attach to growing IFs (arrowheads). Assembly was for 10 s (*A*) and for1 h (*B*). Bar, 100 nm.

exhibits 18 positions at which it differs from the other three vimentins. Similarly, frog and trout vimentin harbor unique amino acids for which the other three species are identically different (fig. 6). Finally, 22 positions of the two fish vimentins differ identically from the tetrapod vimentins, which are also identical at these sites. The absolute sequence identity is highest in the carboxy-terminal part of coil 2B, where the last 34 amino acid residues are absolutely conserved in vimentin of all four species. Coil 1A is also highly conserved with 80% sequence identity among the four species. In contrast, the proposed linker sequences L1, L12 and L2 are only 50% identical, highlighting their role in establishing unique molecular properties for a particular type of vimentin. Relevant to this point, we have recently shown that small changes within one of the linkers (i.e., insertion of three alanines into linker L1 of human vimentin) totally prevents the altered protein from assembling into distinct ULFs and to associate longitudinally [34]. At present, we do not know how these differentially conserved residues contribute to the distinct structural and functional properties of the various vimentins. It is tempting to speculate that they are engaged in specific molecular interactions involved in building and stabilizing an IF, and thus are 'indicators' for specific features of a particular vimentin filament.

Without dwelling too much on amino acid comparisons, it is evident that the distinct molecular properties of individual IF proteins are determined by several characteristic sequence motifs, particularly when considering desmin sequences. Sequence alignment of both vimentin and desmin from zebrafish, *X. laevis*, chicken, and hamster reveals that, besides the generally conserved amino acid sequences, each type of IF protein harbors unique sequence motifs (fig. 7). For example, at the beginning of coil 2B1, vimentins read FADLSE, whereas desmins read VSDL(N/T)Q. Similarly, in the

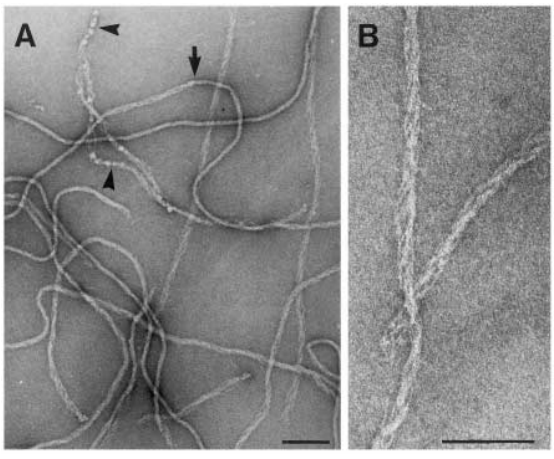

Figure 5. Assembly of *X. laevis* vimentin at 4 °C for 1 h as monitored by electron microscopy of a negatively stained sample Bars, 100 nm. (*A*) Note that long, normal-looking IFs occasionally change into unravelled forms (arrow). In addition, unravelled IFs with (arrowheads) and without bead-like aggregates are found. (*B*) Higher magnification of an open filament exhibiting a right-handed twist.

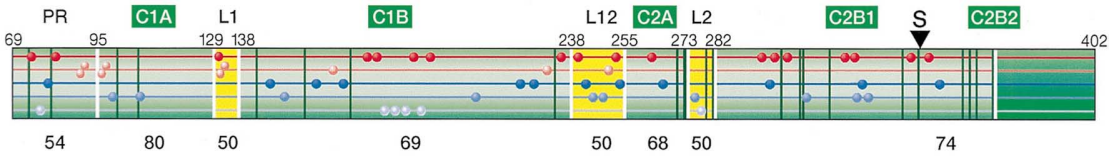

Figure 6. Scheme of the α-helical rod domain of vimentin highlighting various subdomains: PR, precoiled coil region; C1A, coil 1A; L1, linker 1; C1B, coil 1B; L12, linker between coil 1 and coil 2; C2A, coil 2A; L2, linker 2; C2B1, first half of coil 2B with respect to the 'stutter' region S; C2B2, second half of coil 2B. Residues unique in the amino acid sequence of a certain species are depicted as red dots (zebrafish), pink dots (human), dark-blue dots (trout), and light-blue dots (frog, *X. laevis*). The white dots represent identical amino acids in the 'cold' (trout, frog) versus 'warm' (zebrafish, human) vertebrate vimentin sequence. The vertical green bars indicate amino acid positions identical in fish, versus those in the two tetrapods. The numbers above the yellow-colored bars indicate amino acid positions of zebrafish vimentin; the bold numbers below indicate the percentage of amino acid identity of the corresponding subdomain. The dark-green region at the end of coil 2B2 denotes a region with 100% sequence identity between all four species. Note in particular that only those amino acids have been highlighted where the corresponding other three sequences are identically different from the one indicated.

center of coil 1B, desmins are conserved as NNLAA, whereas vimentins are more heterogeneous with a STLQS-type consensus, the character of these amino acid side chains being distinctly different. Besides such extended specific sequence motifs in various positions along the rod, single amino acids differ consistently between the two type III IF molecules. This difference occurs despite the idea that these are somehow equivalent molecules, which (at least in vitro) form heteropolymers indistinguishable from the respective homopolymers [37]. Moreover, in the highly variable head domain, certain features are consistently different. For example, the fifth amino acid of desmin is a tyrosine, and a center of the conserved AM1 motif contains a hydroxy amino acid (Thr). In contrast, vimentin contains a hydrophobic amino acid (Met/Ile) in the latter position. Furthermore, vimentin possesses a cdc2 phosphoacceptor site in its head domain, which is absent in desmin. On the other hand, desmin reveals an SPEQ motif in its tail domain, which is not seen in vimentin. This motif too is a putative phosphoacceptor site for the cdc2 kinase. As a further difference in the head domain, vimentins consistently have two more arginines than desmins. In a peculiarity of the basic head domain, both zebrafish desmin and vimentin exhibit a single glutamic acid up- and downstream of the assembly-relevant motif (AM1). The tail domain, while similar for the two types of IF protein, exhibits various distinct differences between vimentins and desmins.

These sequence differences between vimentin and desmin are clearly manifested in the way they assemble. At room temperature (fig. 8A) and at 37 °C, desmin forms ULFs and IFs that appear to be considerably thicker than those generated by vimentin [20, 34]. In further contrast to vimentin, after 10 s of assembly at 37 °C, desmin ULFs are nearly completely annealed to longer filaments, and ULFs are only encountered occasionally (fig. 8B). Thus, the IF assembly kinetics are considerably faster for desmin than for vimentin [20]. The mass per length (MPL) of these filaments, assembled from recombinant human vimentin and mouse desmin, was determined by STEM mass measurements of unstained/freeze-dried specimens. The differences in MPL of mature IFs are directly compared in figure 9A: vimentin IFs yield MPL peaks of 38, 47, and 56 kDa/nm, whereas desmin filaments exhibit one major peak at 59 kDa/nm.

A MPL histogram very similar to that of recombinant desmin was obtained for authentic chicken gizzard desmin assembled under identical conditions (i.e., dialyzed from 8 M urea into standard assembly buffer); the histogram revealed a relatively sharp and symmetrical peak with 65 kDa/nm, as compared to 59 kDa/nm (fig. 9B). These MPL peaks correspond to 52 and 47 molecules per filament cross-section, respectively. In contrast, chicken gizzard desmin IFs, obtained by dialysis at 4 °C into a buffer of higher pH (but with 5 mM $MgCl_2$), yielded four peaks with 34, 41, 50, and (a small amount) 60 molecules per filament cross-section. This indicated that: (i) desmin forms IFs quite different from those made from vimentin; (ii) with desmin, the number of subunits per filament cross-section is not fixed, but is determined by the exact assembly conditions employed [34].

Molecular models of IF architecture

The above considerations regarding different types of IF assembly justify formulation of a molecular model of IF architecture that allows the coiled-coil dimer to arrange into several distinct types of dimer-dimer inter-

actions and, consequently, introduces 'uncertainty principles,' instead of an 'all for one' model. The classical textbook scheme envisages a surface lattice arrangement involving eight strands, each made of longitudinally associated tetramers. This eight-stranded surface lattice is wrapped into a tubule exhibiting a rather spacious hollow core [38] (fig. 10A). This type of tubular structure, resembling a microtubule, can be excluded based on radial mass density profiles computed from STEM mass measurements [39]. As a consequence, the new edition of Albert et al.'s textbook [40] now favors a model involving seven peripheral and one central fiber. Unfortunately, this new model, while plausible, is not based on state-of-the-art structural data (see below). Another IF model, reproduced in several reviews [7, 8, 41–43], attempts to incorporate the experimental finding that phosphate buffers of low ionic strength mediate partial unravelling of keratin IFs into three to five distinct octameric protofibrils with an apparent diameter of 4.5 nm [32]. While based on an interesting observation, this model too exhibits several inconsistencies. In particular, the way in which the tetramers [shown to be the building blocks for filament assembly; see ref. 20] laterally interact to form the 4.5-nm protofibrils and, ultimately, the entire IF, is far from conclusive. It is clear that the two pairs of dimeric coiled coils within the 4.5-nm protofibril must interact strongly, as more than 5 M urea is required to dissociate the 4.5-nm protofibrils into tetramers. Hence, the geometry of this tetramer-tetramer interaction within the 4.5-nm protofibril has remained elusive [9, 10].

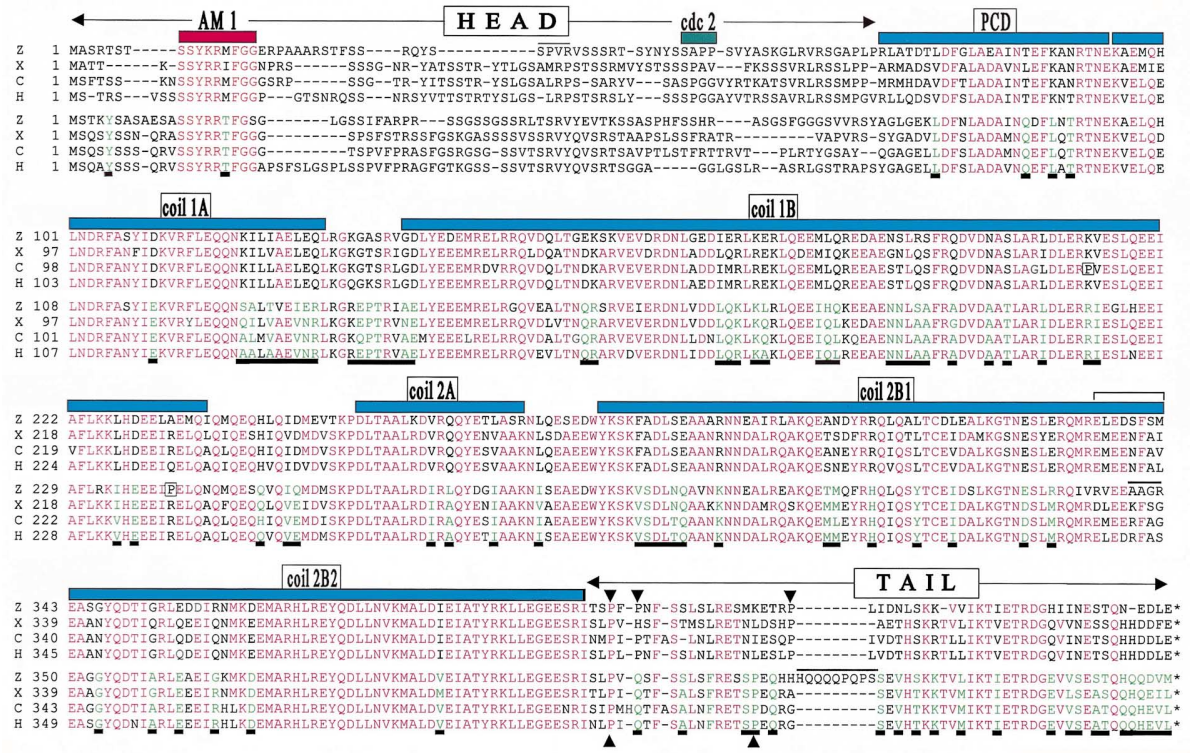

Figure 7. Amino acid sequence comparison of vimentins (upper four rows) versus desmins (lower four rows) from zebrafish (Z), *X. laevis* (X), chicken (C), and hamster (H). Amino acid symbols (one-letter code) are colored red when identical in at least six of the eight sequences. Green letters indicate amino acid positions identical in at least three desmins and different in at least three vimentins. Black bars below the desmin sequences enhance these positions. The non-α-helical N-terminal and C-terminal subdomains are indicated as HEAD and TAIL, respectively. An assembly-relevant motif (AM1) is conserved in the otherwise rather heterogeneous, head domains [see ref. 10]. cdc2 depicts a potential kinase recognition site (SPX +), which in zebrafish is several amino acids upstream, SPVR (overlined). In the tail domain, conserved proline residues are marked by arrowheads: three in vimentin, two in desmin (the second proline could be a potential cdc2 recognition site). PCD, precoiled coil domain (see PR in fig. 6). Helical regions are designated by a blue bar and are named as in fig. 6. The bracket between coil 2B1 and coil 2B2 marks the 'stutter' region. In zebrafish desmin, this region deviates considerably from the other desmin sequences (overlined). Also, in the tail domain, zebrafish exhibits a major insertion compared to the other three sequences (overlined).

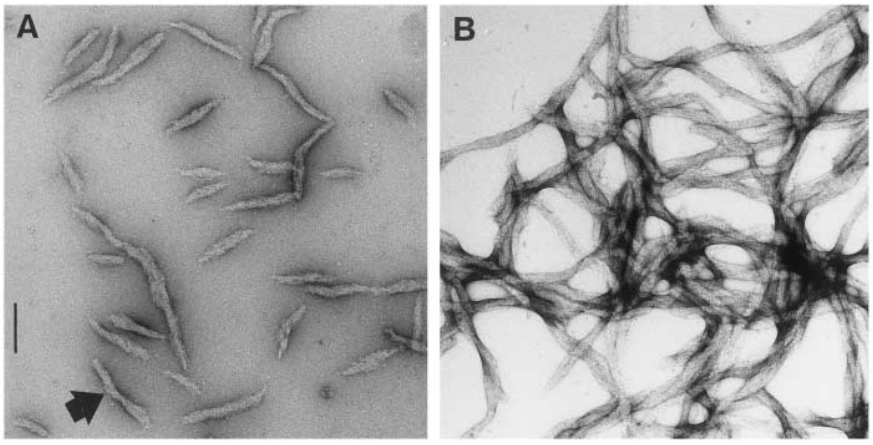

Figure 8. Electron microscopic analysis of negatively stained human desmin filaments, formed 10 s after initiation of assembly at room temperature (*A*) or 37 °C (*B*). The large arrow in (*A*) denotes a discontinuity, indicative of two filaments evidently in the process of longitudinal annealing. Bar, 100 nm.

Thus, based on the observation that tetrameric complexes, reconstituted from urea-denatured protein by dialysis into buffers of low ionic strength and high pH [44], are stable and do not significantly associate under these conditions, we have argued that the three-dimensional arrangement of the two dimeric coiled coils within a tetramer must be trapped in a non-productive conformation. Structural rearrangements probably have to occur within this tetrameric complex when IF assembly is initiated by a 'kinetic-type assembly' regimen [9]. Hence, the abrupt increase in ionic strength and the rapid drop of pH (by 1 unit) must release the 'assembly block' of the urea (low ionic strength/high pH)-reconstituted tetramers, possibly by overcoming the non-productive binding of several of the basic residues of the non-helical head domain to the rod. Now free to interact with neighboring tetramers, these positively charged head domains could quickly mediate the tight lateral association of eight tetramers into an ULF. In a next step, ULFs anneal longitudinally into filaments exhibiting an unusually large diameter (i.e., 16–23 nm). Finally, after several minutes these 'immature' filaments appear to laterally 'compact,' to yield 'mature' IFs with an apparent diameter of 11–13 nm. This reduction in filament diameter is 'conservative' in the sense that the MPL, as determined by STEM comparing immature and mature filament measurements, remains unchanged. This strongly argues for an intrafilamentous rearrangement of dimers and/or tetramers [34].

The non-α-helical 'head' domain is essential for the generation of IF assembly tetramers, since headless cytokeratins (as well as headless vimentins) are unable to laterally associate beyond the coiled-coil dimers [20, 45]. In line with this behavior, both vimentin and desmin with proteolytically shortened or point-mutated head domains fail to assemble properly into bona fide IFs [16, 17, 46]. Evidently, the relative positioning of the two coiled coils within the tetramer (i.e., in terms of relative polarity and stagger) determines the type and degree of lateral and longitudinal tetramer-tetramer interaction within the mature IF. Cross-linking experiments with tetramers have revealed that one major dimer-dimer interaction involves coil 1B associating in an antiparallel, approximately half-staggered orientation, yielding $\sim$65-nm-long tetrameric complexes [47] designated the A_{11} form (fig. 11) [8]. In cross-section, the packing of α-helices in the tetramer could form a square or a parallelogram. We favor a parallelogram organization, because it would allow closer packing of α-helices and consequently an IF with minimal hollow core [see fig. 10A; for comparison see ref. 9]. This type of dimer-dimer interaction, in turn, would result in a minimal-size hollow core and, additionally, allow for dynamic changes of some of the lateral interactions between tetrameric complexes within the filament (fig. 10C) [9].

A quite different mode of subunit interaction has been proposed by Downing [48], suggesting the establishment of a central hydrophobic channel formed by a hydrophobic seam extending along each α-helix from the amino acids in the a and d positions of the heptad repeats. This mode of subunit interaction implies that no two-stranded α-helical coiled-coil dimers would form. However, there is no experimental evidence to support such a molecular arrangement. Furthermore, our model proposes that the head domains of at least

half of the polypeptides should be exposed to the outside of the filament. In the case of vimentin, this would generate a 'garland' of 12×16 (i.e., 192) arginines evenly distributed over the surface of a 43-nm-long filament stretch, and another 192 arginines within the central core of the filament. Probably, most of these arginines bind to charged residues on the surface of the filament shaft, thus contributing to the known stability of IFs at high ionic strength (as high as 1.5 M KCl). In contrast, at low ionic strength, IFs tend to depolymerize indicating that closely spaced repulsive charges are becoming dominant. Moreover, multivalent anions such as phosphate have been shown to specifically interfere with the keratin IF structure, leading to a partial unravelling of the filament backbone into protofilaments or protofibrils [32]. This directly leads to considerations of quasi-equivalence for (at least some of) the lateral dimer-dimer interactions occurring in mature IFs [9].

Finally, the situation becomes even more complex if heteropolymer formation is considered. In the case of cytokeratin IFs, type I and type II subunits are required to form obligatory heterodimers, which then further associate to yield heterotypic tetramers [49–51]. Second, neurofilaments are composed of three sequence-related polypeptides, the neurofilament triplet proteins of low, medium, and high molecular weight (NF-L, NF-M, and NF-H). Besides the NF-L/NF-L homodimers, heterodimers composed of NF-L/NF-M and NF-L/NF-H are the most favored species that may differentially associate, eventually forming the mature neurofilament [52–54]. Third, the beaded-chain filaments of eye lens fiber cells, composed of two unusually structured IF proteins, phakinin (CP49) and filensin, probably assemble in a similar way to neurofilaments. More specifically, these filaments may consist of a 'core filament' made from four phakinin tetramers per cross-section, which further associates with four heterotetramers made from phakinin/filensin heterodimers (fig. 10D) [55–57]. Although this molecular architecture, proposed for the beaded chain filaments (fig. 10D), may also hold true for other IF proteins (such as the neurofilament triplet proteins, nestin, synemin, and paranemin), the exact in vivo assembly pathway (which may also pertain to vimentin, desmin, or other IF proteins) remains elusive [58–60].

Some of the molecular features leading to IF polymorphism

Parry and Steinert [8] pointed out that four types of IF proteins can be discerned with regard to their 'near-axial periodicity.' Epidermal ('soft') cytokeratins exhibit values of 22.7 nm, which are significantly different from hair ('hard') α-keratins with an axial repeat of 23.5 nm. Vimentin (and possibly the other type III and IV IF proteins) exhibit 21.3-nm repeats. Nuclear lamins and invertebrate cytoplasmic IF proteins (that share a 42-amino-acid insertion in coil 1B) exhibit an axial repeat pattern of 24–25 nm. These distinct structural parameters imply unique assembly characteristics of these proteins, preventing significant co-polymerization of members from these four different groups. Ultimately, these distinct molecular properties may determine how

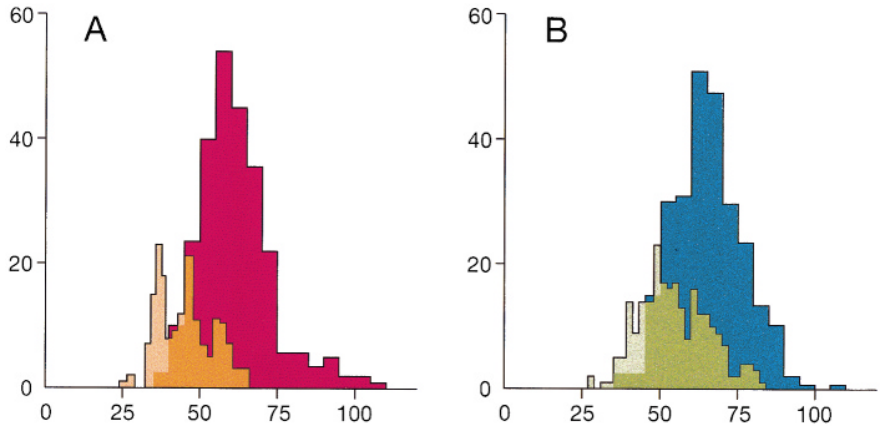

Figure 9. Histograms of MPL measurements of recombinant desmin IFs compared to recombinant vimentin IFs (*A*), and chicken gizzard desmin IFs assembled under different conditions (*B*). Abscissa, MPL (kDa/nm); ordinate, number of filament segments measured. (*A*) Vimentin (yellow) and desmin (red) IFs were formed in the kinetic mode (i.e., addition of buffered salt solution) at 37 °C for 1 h. (*B*) Chicken gizzard desmin IFs were either assembled in the kinetic mode at 37 °C for 1 h (blue) or by overnight dialysis into a buffer containing $MgCl_2$ at 4 °C (green).

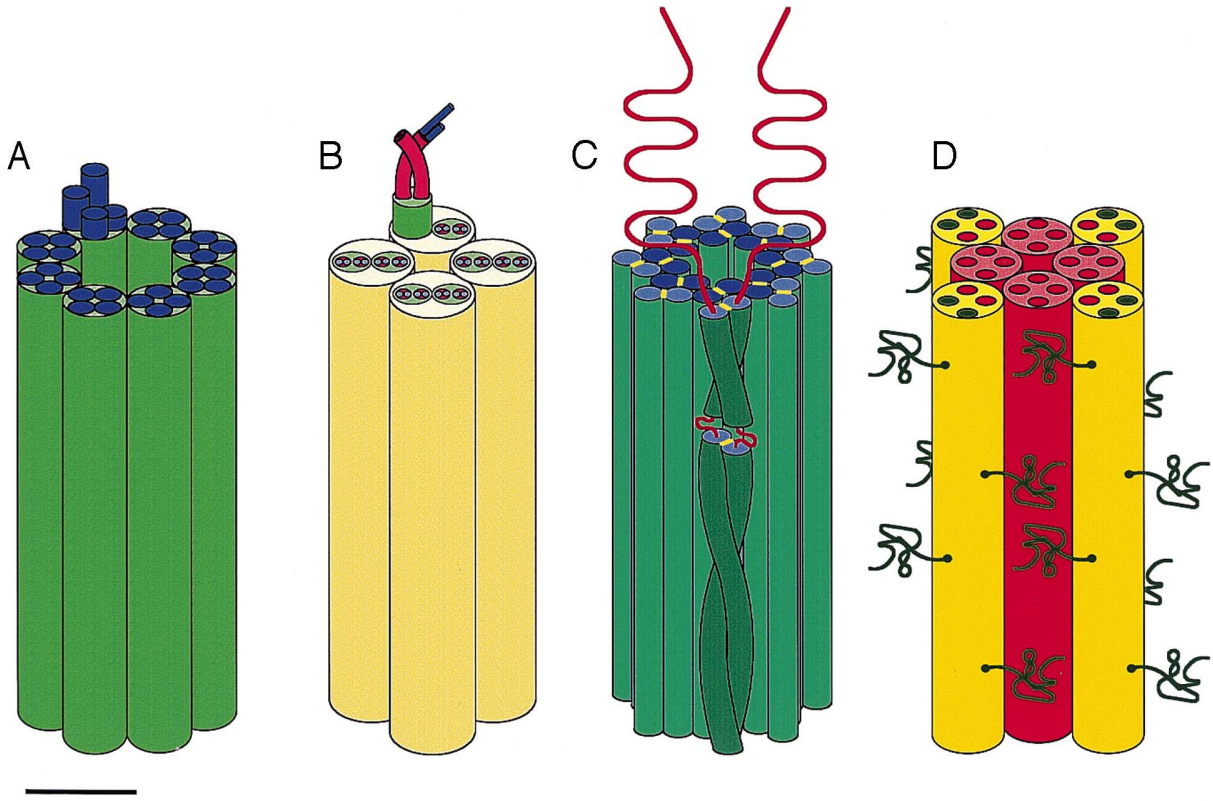

Figure 10. Different models of IF subunit arrangements. The models are highly schematic. Individual protofilaments and protofibrils are helicoidally twisted. Bar, 5 nm. (*A*) This model favors a tube with radial symmetry made from eight individual protofilaments (green cylinders), each consisting of longitudinally interacting tetrameric complexes of individual α-helices (blue tubes) [redrawn from ref. 38]. As indicated in the model, this type of subunit arrangement would yield a pronounced hollow core. (*B*) The main building blocks according to this model [redrawn from ref. 42] are the octameric protofibrils (yellow cylinders), each consisting of two tetrameric protofilaments (green cylinders). The protofibrils are assumed to be ca 4.5 nm in diameter. It is hard to reconcile how eight α-helical molecules (blue tubes), each with an approximate diameter of 1 nm, could fit in the depicted orientation into a 4.5-nm protofibril. (*C*) The basic subunit of an IF, the antiparallel tetramer is shown as a 'closest'-packed unit, with dark- and light-blue cross-sections indicating α-helices packaged in a coiled coil by hydrophobic forces (yellow bars). Eight such tetrameric subunits are packed together as closely and as symmetrically as possible [see ref. 9], thereby generating a minimal-size hollow core. In this model, we try to keep individual subunits to scale, thereby approximating a 10-nm filament built from 2-nm dimeric coiled coils and 2.8-nm-diameter tetramers. The coil 1 segments of one of the coiled coils (in the front) is schematically drawn with a helical pitch of 14 nm and the interruption through linker L1 (red loops between the helically twisted tubes). The red structures at the top (shown for one dimer) represent the non-helical amino-terminal ('head') domains which may be distinctively structured, because of stacking of six aromatic side chains [see ref. 10]. (*D*) Model for a beaded-chain IF consisting of two different IF proteins: phakinin (red) and filensin (green) in a proportion of 3:1. The exact arrangement of the heteropolymeric complexes (yellow tubes) is not known. However, the long non-α-helical C-terminal 'tail' domains of filensin probably stick out of the filament [redrawn from ref. 55].

many tetramers can preferentially aggregate laterally into a filament, thus explaining why IF proteins of individual sequence homology classes contain different numbers of molecules per filament cross-section and, consequently, yield different MPL values [34]. Remarkably, the largest differences with respect to their MPLs have been observed comparing desmin and vimentin, two type III sequence homology class members with high sequence identity [34]. In contrast, while vimentins from different species (such as human and frog) exhibit similar values of overall sequence identity [as do human vimentin and human desmin, i.e., around 72%; see ref. 33], they reveal very similar MPL values [20]. Hence, some rather subtle sequence motifs, characteristic for a particular IF protein type (see fig. 7), must ultimately be responsible for these relatively large differences in MPL. The importance of such IF protein type-specific sequence motifs is exemplified by the cytoplasmic IF proteins of invertebrates. As mentioned above, they possess (like nuclear lamins) a 42-amino-acid insertion

in coil 1B, and yet exhibit a different mode of filament assembly. They form tetramers rather than dimers as in the case of nuclear lamins. They first associate head-to-tail before significant lateral association occurs, to yield mature IFs appearing similar to vertebrate IFs [61]. Their MPL values are in the range of vertebrate IFs, as determined for *Ascaris* proteins (high and low) which exhibit a major MPL value of 37 kDa/nm, with additional peaks at 59, 77, and 94 kDa/nm. More subtle functional assays may eventually provide information on how similar they are to vertebrate IF proteins.

The dilemma of missing quantitative data

To achieve a model of the IF in which every dimeric coil 1 domain is adjacent to a dimeric coil 2 domain [as detected from cross-linking experiments; see ref. 8], three types of tetramer, A_{11}, A_{12}, and A_{22} (see fig. 11), would have to associate with each other via coil 1/coil 2 interactions. For efficient ULF formation, appropriate amounts of all three types of tetramer should be present. However, analysis of soluble vimentin oligomers by analytical ultracentrifugation has revealed that octameric species are also present, although it is not known how they are formed or how many different types exist (fig. 11) [9, 20]. In principle, two types of tetramer interaction to generate an octameric complex are conceivable and compatible with the structural IF model proposed by Fraser et al. [62]: (i) a tetramer of the A_{11} type may associate with one of the A_{22} type, via interaction of a coil 1 dimer with the corresponding coil 2 dimer (fig. 11; A_{11}/A_{22}); (ii) two tetramers of the A_{12} type may interact via a coil 1 dimer in an antiparallel, half-staggered fashion (fig. 11; A_{12}/A_{12}). Whether any of these octameric complexes represent the active species for productive assembly is not known. We also do not

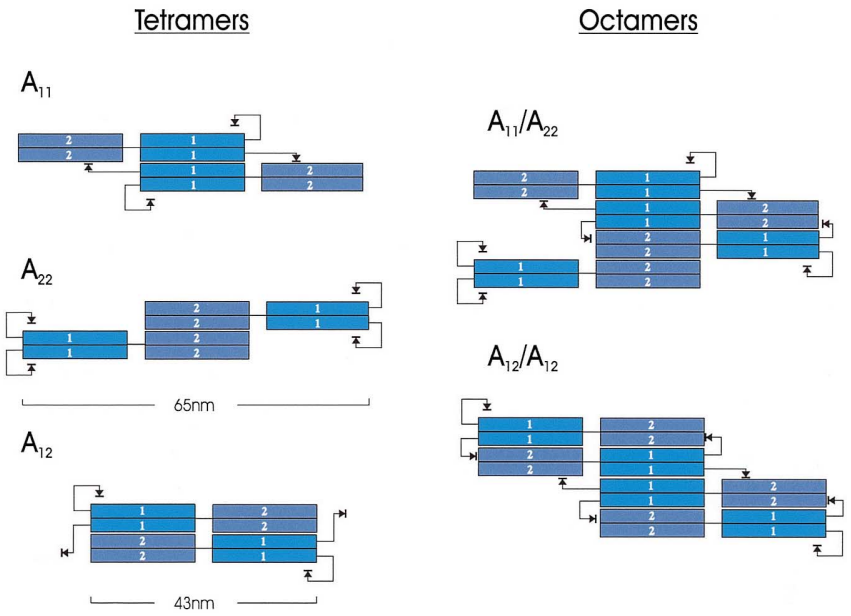

Figure 11. Schematic representation of tetramers (left panel) and octamers (right panel). The A_{11} tetramer represents an antiparallel, approximately half-staggered complex of two coiled-coil dimers interacting through their coil 1 domains (light-blue boxes), the A_{22} tetramers are the corresponding complex generated by interaction of their coil 2 domains (dark-blue boxes). An antiparallel, unstaggered interaction of two dimers would result in the A_{12} teramer. The A_{11} and A_{22}, and A_{12} tetramers have been calculated to measure approximately 65 nm and 43 nm, respectively [8]. The hypothetical interaction of an A_{11}-type with an A_{22}-type tetramer through their coil 1 and coil 2 domains would generate an octamer of 65 nm (A_{11}/A_{22}). Correspondingly, the interaction of two A_{12} tetramers through their coil 1 domains could also generate an octameric complex (A_{12}/A_{12}) of 65 nm [compare with Fig. 3.17, p. 93, in ref. 8]. Note that four oligomers of both the (A_{11}/A_{22}) and the (A_{12}/A_{12}) type could laterally aggregate to form an ULF of identical molecular composition and would therefore be able to longitudinally fuse with one another. The non-helical amino-terminal domains ('heads') are indicated by arrows. Since the mode of their interaction with the α-helical rod domains is not known, we have arbitrarily indicated potential binding regions on coil 1 and coil 2. However, since headless vimentins and cytokeratins form dimers but not tetramers [20, 45], the head domains are likely to be engaged in tetramer formation. Therefore, it is hard to reconcile how the A_{22} tetramers could form, since their head domains are rather distantly located from the interacting coil 2 domains. The visualization of tetramers/octamers by glycerol spraying/rotary-metal-shadowing electron microscopy establishes the existence of extended rodlike particles of 45 and 65 nm in length [20].

know the relative amounts of the different tetramer species present, nor the dynamics of conversion from one type to another. In principle, the A_{12} tetramer could be the active species, so that two of them would associate to form an approximately half-staggered antiparallel octamer (fig. 11; A_{12}/A_{12}), and four of these octamers could join laterally to yield the ULF [9]. 'Tetramer switching' of the A_{11} and the A_{22} species [4] could replenish the A_{12} tetramer as it is consumed for octamer formation. Collision-type interactions between tetramers have been excluded, based on cross-linking experiments of various engineered vimentins (fig. 7) [63]. Therefore, conversion of an A_{11} tetramer into an A_{12} tetramer, for example, has to be the result of a rearrangement within a tetramer [4].

The situation becomes even more complex when data obtained by transient electric birefringence measurements are considered. Employing this method, Kooijman and colleagues [64] found that vimentin (in 5 mM Tris-HCl, pH 8.5) occurs as a heterodisperse mixture of particles of different size, revealing two decay processes. At pH 6.8, three components were observed. Thus, these authors conclude that considerable amounts of hexamers [compare with ref. 50], were present side by side with antiparallel staggered tetramers and octamers. In addition, they postulated the existence of dimers, which have never been encountered under these buffer conditions in any significant amount by analytical ultracentrifugation [20]. The types of intermediates formed when assembly is initiated with such a heterogeneous mixture of soluble oligomers may increase significantly and give rise to the MPL polymorphism, observed even along one and the same filament (fig. 9) [20]. Similarly, Steinert [50 and references therein] followed the occurrence of increasingly complex oligomers with cytokeratins 1 and 10 in a buffer system that yields a low assembly rate, so that little polymer is detected within the first 12 min after initiation of assembly. This is in marked contrast to the behavior of cytokeratins 8 and 18, which by 5 min of assembly reached nearly maximal values of viscosity, indicating that long filaments had formed by that time [65]. Moreover, the assembly of cytokeratin 8 with different acidic partners (i.e., CK13, 18, 19, or 20) revealed that at 5 mM Tris-HCl, CK20 was by far the best assembly partner for CK8. In addition, the four different pairs of CKs generated IFs that looked quite different by electron microscopy of negatively stained samples [65]. Hence, one may speculate that the subunit number per cross-section of CK8/13, CK8/19 and CK8/20 appears to be significantly different from that of CK8/18 IFs.

One reason for the observed differences with the data obtained for CK1/10 IFs might result from the fact that Steinert [50] used protein isolated from murine epidermis, which may have been posttranslationally modified in this terminally differentiated tissue, in such a way that the dynamics of assembly or even the subunit composition were affected. Similarly, bovine lens vimentin, which is stably deposited in a highly ordered state in the terminally differentiated lens fiber cells [57], assembles much more slowly than bacterially expressed human vimentin, although both vimentins have nearly identical amino acid sequences, suggesting some type of posttranslational modification modulating assembly [31, 66, 67]. In analogy to the different assembly behavior of vimentin and desmin [34], it is also conceivable that different cytokeratin pairs form significantly different types of IFs, since their amino acid sequences are much less conserved than those of desmin and vimentin. This is especially true when a pair such as CK8/18 and CK1/10 are compared (e.g., the rod of human CK1 and 8 is 64.1%, that of CK10 and 18 only 51.1%, and that of desmin and vimentin 73.5% identical). Moreover, as shown for vimentin, the assembly regimen and the physiological parameters employed are of critical importance to the structure and MPL distribution of the growing IFs. This will probably also hold true for most other IF proteins [20, 67].

Conclusions and perspectives

Polymorphism of distinct biological assemblies may, at first glance, irritate structural biophysicists [8]. However, this is not a new scenario. The emergence of distinct types of filaments from one seemingly identical kind of molecule has previously been observed with both actin filaments [68] and with microtubules [69 and references therein]. Rather, the ability of a particular filament protein to form distinct supramolecular assemblies may be of physiological significance. The fine-tuned response of an IF protein (such as vimentin) to temperature and its interaction with heat shock proteins [31, 70] points to a potentially important functional property acquired during evolution [71].

Recent studies on skin diseases have clearly demonstrated that single amino acid changes in specific IF proteins have direct clinical sequelae, as in the case of the various forms of epidermolysis bullosa simplex or epidermolytic hyperkeratosis [42]. Thus, it is beyond doubt that cytokeratin-type IFs have a distinct function with regard to the mechanical integrity of cells. Moreover, the large variety of cytokeratin proteins found supports the notion that a single type of IF protein cannot satisfy the needs of various tissues. Indeed, new cytokeratins are still being identified, sometimes leading to the elucidation of new types of cells that were not previously distinguished from neighboring cells [see ref. 72 for a novel human type II cytokeratin, K6hf, in the companion layer of the hair follicle]. Furthermore, the

role of CK16 in wound repair is far from being understood. It is not even known if more than one CK16 gene is present in humans [73, 74].

An even more dramatic impact on tissue architecture has been described in the case of IF protein gene inactivation, such as the muscle-specific IF protein desmin. The absence of this hallmark cytoskeletal protein within the sarcomere is fatal for homozygous transgenic animals, due to serious deteriorations in the structure of the beating heart myoblasts [75]. In addition, recent analyses of 'knockout' mice (negative for the simple epithelial-type cytokeratins CK8 and 18) demonstrate phenotypes which go beyond mere structural defects. For example, the hepatocytes of such mice degenerate severely upon aging, exhibiting necrotic foci, hepatomegaly, and massive tissue infiltration of red blood cells [76]. Moreover, the exchange of a phosphoacceptor serine for an alanine in the non-helical head domain of cytokeratin 18 in transgenic mice renders these animals extremely sensitive to hepatotoxins [77]. Although neither the filament organization nor the ability of their livers to regenerate after partial hepatectomy is affected by the co-expression of the mutated cytokeratin, cellular physiology is apparently influenced in a dramatic way. Hence, IF proteins may be of importance for cellular homeostasis combating cellular stress events, such as those encountered during viral infections, apoptosis, and challenges by toxins.

Obviously, mechanical stress is only one type of insult with which eukaryotic cells and tissues must cope. Hence, it is an attractive possibility that during the evolution of a specific animal species, various IF proteins have acquired distinct functions within the particular tissue in which they are expressed. Indeed, some of these specific functions may not be related exclusively to the filamentous appearance of IF proteins but may be related to alternative structures that might be adopted under certain physiological conditions.

Acknowledgements. We cordially thank Monika Brettel, Markus Häner, and Ariel Lustig for their excellent technical assistance over the past years. Sabine Reichel-Klingmann is thanked for efficient secretarial assistance, Jutta Osterholt for photographic artwork, and Ralf Zimbelmann for numerous sequence alignments. In particular, we want to thank Dr. Ansgar Schmidt and Robert Wyss for generating the computer graphics shown in this manuscript. Special thanks go to Drs. Ada and Don Olins for critical reading of the text. Dr. Werner W. Franke is thanked for his continuous interest and support. Financial support by the German Research Foundation (DFG) and the 'Förderprogramm der Gemeinsamen Forschungskommission der Medizinischen Fakultät Heidelberg' (to H. H.), as well as the Swiss National Science Foundation and the M. E. Mueller Foundation of Switzerland (to U. A.) are gratefully acknowledged.

1 Kabsch W., Mannherz H. G., Suck D., Pai E. F. and Holmes K. C. (1990) Atomic structure of the actin:DNase I complex. Nature **347:** 37–44

2 Lowe J. and Amos L. A. (1998) Crystal structure of the bacterial cell-division protein FtsZ. Nature **391:** 203–206

3 Nogales E., Wolf S. G. and Downing K. H. (1998) Structure of the $\alpha\beta$ tubulin dimer by electron crystallography. Nature **391:** 199–203

4 Aebi U., Häner M., Troncoso J., Eichner R. and Engel A. (1988) Unifying principles in intermediate filament (IF) structure and assembly. Protoplasma **145:** 73–81

5 Stewart M. (1993) Intermediate filament structure and assembly. Curr. Opin. Cell Biol. **5:** 3–11

6 Heins S. and Aebi U. (1994) Making heads and tails of intermediate filament assembly, dynamics and networks. Curr. Opin. Cell Biol. **6:** 25–33

7 Fuchs E. and Weber K. (1994) Intermediate filaments: structure, dynamics, function, and disease. Annu. Rev. Biochem. **63:** 345–382

8 Parry D. A. D. and Steinert P. M. (1995) Intermediate Filament Structure, Springer, Berlin

9 Herrmann H. and Aebi U. (1998) Intermediate filament assembly: fibrillogenesis is driven by decisive dimer-dimer interactions. Curr. Opin. Struct. Biol. **8:** 177–185

10 Herrmann H. and Aebi U. (1998) Structure, assembly and dynamics of intermediate filaments. In: Intermediate Filaments: Subcellular Biochemistry, vol. 31, pp. 319–362, Herrmann H. and Harris J. R. (eds.), Plenum, New York

11 Miller R. K., Khuon S. and Goldman R. D. (1993) Dynamics of keratin assembly: exogenous type I keratin rapidly associates with type II keratin in vivo. J. Cell Biol. **122:** 123–135

12 Stuurman N., Heins S. and Aebi U. (1998) Nuclear lamins: their structure, assembly, and interactions. J. Struct. Biol. **122:** 42–66

13 Markl J. and Schechter N. (1998) Fish intermediate filament proteins in structure, evolution, and function. In: Intermediate Filaments: Subcellular Biochemistry, vol. 31, pp. 1–33, Herrmann H. and Harris J. R. (eds.), Plenum, New York

14 Riemer D. and Weber K. (1998) Common and variant properties of intermediate filament proteins from lower chordates and vertebrates: two proteins from the tunicate *Styela* and the identification of a type III homologue. J. Cell Sci. **111:** 2967–2975

15 Herrmann H., Fouquet B. and Franke W. W. (1989) Expression of intermediate filament proteins during development of *Xenopus laevis*. II. Identification and molecular characterization of desmin. Development **105:** 299–307

16 Raats J. M. H., Pieper F. R., Vree Egberts W. T. M., Verrijp K. N., Ramaekers F. C. S. and Bloemendal H. (1990) Assembly of amino-terminally deleted desmin in vimentin-free cells. J. Cell Biol. **111:** 1971–1985

17 Herrmann H., Hofmann I. and Franke W. W. (1992) Identification of a nonapeptide motif in the vimentin head domain involved in intermediate filament assembly. J. Mol. Biol. **223:** 637–650

18 Hofmann I. and Herrmann H. (1992) Interference in vimentin assembly in vitro by synthetic peptides derived from the vimentin head domain. J. Cell Sci. **101:** 687–700

19 Hatzfeld M., Dodemont H., Plessmann U. and Weber K. (1992) Truncation of recombinant vimentin by ompT: identification of a short motif in the head domain necessary for assembly of type III intermediate filament proteins. FEBS Lett. **302:** 239–242

20 Herrmann H., Häner M., Brettel M., Müller S. A., Goldie K. N., Fedtke B. et al. (1996) Structure and assembly properties of the intermediate filament protein vimentin: the role of its head, rod and tail domains. J. Mol. Biol. **264:** 933–953

21 Helfman G. S., Collette B. B. and Facey D. E. (1997) The Diversity of Fishes, Blackwell, Oxford

22 Franke W. W. (1987) Nuclear lamins and cytoplasmic intermediate filament proteins: a growing multigene family. Cell **48:** 3–4

23 Janmey P., Shah J. V. and Janssen K.-P. (1998) Viscoelasticity of intermediate filament networks. In: Intermediate Filaments: Subcellular Biochemistry, vol. 31, pp. 381–397, Herrmann H. and Harris J. R. (eds.), Plenum, New York

24 Borisy G. G., Olmsted J. B., Marcum J. M. and Allen C. (1974) Microtubule assembly in vitro. Fed. Proc. **33:** 167–174
25 Starger J., Brown W. E., Goldmann A. E. and Goldman R. D. (1978) Biochemical and immunological analysis of rapidly purified 10 nm filaments from baby hamster kidney (BHK-21) cells. J. Cell Biol. **78:** 93–109
26 Schliwa M. and Euteneuer U. (1979) Structural transformation of epidermal tonofilaments upon cold treatment. Exp. Cell Res. **122:** 93–101
27 Fox H. and Whitear M. (1986) Genesis and regression of the figures of Eberth and occurrence of cytokeratin aggregates in the epidermis of anuran larvae. Anat. Embryol. **174:** 73–82
28 Franke W. W., Schmid E., Grund C. and Geiger B. (1982) Intermediate filament proteins in nonfilamentous structures: transient disintegration and inclusion of subunit proteins in granular aggregates. Cell **30:** 103–113
29 Rosevear E. R., McReynolds M. and Goldman R. D. (1990) Dynamic properties of intermediate filaments: disassembly and reassembly during mitosis in baby hamster kidney cells. Cell Motil. Cytoskeleton **17:** 150–166
30 Eckelt A., Herrmann H. and Franke W. W. (1992) Assembly of a tail-less mutant of the intermediate filament protein, vimentin, in vitro and in vivo. Eur. J. Cell Biol. **58:** 319–330
31 Herrmann H., Eckelt A., Brettel M., Grund C. and Franke W. W. (1993) Temperature-sensitive intermediate filament assembly alternative structures of *Xenopus laevis* vimentin in vitro and in vivo. J. Mol. Biol. **234:** 99–113
32 Aebi U., Fowler W. E., Rew P. and Sun T.-T. (1983) The fibrillar substructure of keratin filaments unravelled. J. Cell Biol. **97:** 1131–1143
33 Herrmann H., Münick M. D., Brettel M., Fouquet B. and Markl J. (1996) Vimentin in a cold-water fish, the rainbow trout: highly conserved primary structure but unique assembly properties. J. Cell Sci. **109:** 569–578
34 Herrmann H., Häner M., Brettel M., Nam-On K. and Aebi U. (1999) Characterization of distinct early assembly units of different intermediate filament proteins. J. Mol. Biol. **286:** 1403–1420
35 Cerdà J., Conrad M., Markl J., Brand M. and Herrmann H. (1998) Zebrafish vimentin: molecular characterization, assembly properties and developmental expression. Eur. J. Cell Biol. **77:** 175–187
36 Morley S. M., Dundas S. R., James J. L., Gupta T., Brown R. A., Sexton C. J. et al. (1995) Temperature sensitivity of the keratin cytoskeleton and delayed spreading of keratinocyte lines derived from EBS patients. J. Cell Sci. **108:** 3463–3471
37 Steven A. C., Wall J., Hainfeld J. and Steinert P. M. (1982) Structure of fibroblastic intermediate filaments: analysis by scanning transmission electron microscopy. Proc. Natl. Acad. Sci. USA **79**: 3101–3105
38 Alberts B., Bray D., Lewis J., Raff M., Roberts K. and Watson J. D. (1994) Molecular Biology of the Cell, 3rd edn, Garland, New York
39 Steven A. C. (1990) Intermediate filament structure: diversity, polymorphism, and analogy to myosin. In: Cellular and Molecular Biology of Intermediate Filaments, pp. 233–263, Goldman R. D. and Steinert P. M. (eds.), Plenum, New York
40 Alberts B., Bray D., Johnson A., Lewis J., Raff M., Roberts K. et al. (1998) Essential Cell Biology, Garland, New York
41 Fuchs E. (1994) Intermediate filaments and disease: mutations that cripple cell strength. J. Cell Biol. **125:** 511–516
42 Fuchs E. (1995) Keratins and the skin. Annu. Rev. Cell Dev. Biol. **11:** 123–153
43 Fuchs E. and Cleveland D. W. (1998) A structural scaffolding of intermediate filaments in health and disease. Science **279:** 514–519
44 Renner W., Franke W. W., Schmid E., Geisler N., Weber K. and Mandelkow E. (1981) Reconstitution of intermediate-sized filaments from denatured monomeric vimentin. J. Mol. Biol. **149:** 285–306
45 Hatzfeld M. and Burba M. (1994) Function of type I and type II keratin head domains: their role in dimer, tetramer and filament formation. J. Cell Sci. **107:** 1959–1972
46 Traub P. and Vorgias C. E. (1983) Involvement of the N-terminal polypeptide of vimentin in the formation of intermediate filaments. J. Cell Sci. **63:** 43–67
47 Geisler N., Schünemann J. and Weber K. (1992) Chemical cross-linking indicates a staggered and antiparallel protofilament of desmin intermediate filaments and characterizes one higher-level complex between protofilaments. Eur. J. Biochem. **206:** 841–852
48 Downing D. T. (1996) Chemical cross-linking between lysine groups in vimentin oligomers is dependent on local peptide conformations. Proteins Struct. Funct. Genet. **25:** 215–224
49 Hatzfeld M. and Weber K. (1990) The coiled coil of in vitro assembled keratin filaments is a heterodimer of type I and II keratins: use of site-specific mutagenesis and recombinant protein expression. J. Cell Biol. **110:** 1199–1210
50 Steinert P. M. (1991) Analysis of the mechanism of assembly of mouse keratin 1/keratin 10 intermediate filaments in vitro suggests that intermediate filaments are built from multiple oligomeric units rather than a unique tetrameric building block. J. Struct. Biol. **107:** 175–188
51 Coulombe P. A. and Fuchs E. (1990) Elucidating the early stages of keratin filament assembly. J. Cell Biol. **111:** 153–169
52 Heins S., Wong P. C., Müller S., Goldie K., Cleveland D. W. and Aebi U. (1993) The rod domain of NF-L determines neurofilament architecture, whereas the end domains specify filament assembly and network formation. J. Cell Biol. **123:** 1517–1533
53 Cohlberg J. A., Hajarian H., Tran T., Alipourjeddi P. and Noveen A. (1995) Neurofilament protein heterotetramers as assembly intermediates. J. Biol. Chem. **270:** 9334–9339
54 Leung C. L., Flores R. L. and Liem R. K. H. (1998) The complexity of intermediate filaments in the nervous system. In: Intermediate Filaments: Subcellular Biochemistry, vol. 31, pp. 497–526, Herrmann H. and Harris J. R. (eds.), Plenum, New York
55 Goulielmos G., Gounari F., Remington S., Müller S., Häner M., Aebi U. et al. (1996) Filensin and phakinin form a novel type of beaded intermediate filament and coassemble de novo in cultured cells. J. Cell Biol. **132:** 643–655
56 Georgatos S. D., Gounari F., Goulielmos G. and Aebi U. (1997) To bead or not to bead? Lens-specific intermediate filaments revisited. J. Cell Sci. **110:** 2629–2634
57 Sandilands A., Masaki S. and Quinlan R. A. (1998) Lens intermediate filament proteins. In: Intermediate Filaments: Subcellular Biochemistry, vol. 31, pp. 291–318, Herrmann H. and Harris J. R. (eds.), Plenum, New York
58 Bilak S. R., Sernett S. W., Bilak M. M., Bellin R. M., Stromer M. H., Huiatt T. W. et al. (1998) Properties of the novel intermediate filament protein synemin and its identification in mammalian muscles. Arch. Biochem. Biophys. **355:** 63–76
59 Marvin M. J., Dahlstrand J., Lendahl U. and McKay R. D. (1998) A rod end deletion in the intermediate filament protein nestin alters its subcellular localization in neuroepithelial cells of transgenic mice. J. Cell Sci. **111:** 1951–1961
60 Hemken P. M., Bellin R. M., Sernett S. W., Becker B., Huiatt T. W. and Robson R. M. (1997) Molecular characteristics of the novel intermediate filament protein paranemin. J. Biol. Chem. **272:** 32489–32499
61 Geisler N., Schünemann J., Weber K., Häner M. and Aebi U. (1998) Assembly and architecture of invertebrate cytoplasmic intermediate filaments reconcile features of vertebrate cytoplasmic and nuclear lamin-type intermediate filaments. J. Mol. Biol. **282:** 601–617
62 Fraser R. D. B., MacRae T. P. and Parry D. A. D. (1990) The three-dimensional structure of IF. In: Cellular and Molecular Biology of Intermediate Filaments, pp. 205–231, Goldman R. D. and Steinert P. M. (eds.), Plenum, New York
63 Rogers K. R., Herrmann H. and Franke W. W. (1996) Characterization of disulfide crosslink formation of human vimentin at the dimer, tetramer, and intermediate filament levels. J. Struct. Biol. **117:** 55–69

64 van Amerongen H., Kooijman M. and Bloemendal M. (1998) Transient electric birefringence in the study of intermediate filament assembly. In: Intermediate Filaments: Subcellular Biochemistry, vol. 31, pp. 399–421, Herrmann H. and Harris J. R. (eds.), Plenum, New York
65 Hofmann I. and Franke W. W. (1997) Heterotypic interactions and filament assembly of type I and type II cytokeratins in vitro: viscometry and determinations of relative affinities. Eur. J. Cell Biol. **72:** 122–132
66 Hess J. F., Casselman J. T. and FitzGerald P. G. (1994) Nucleotide sequence of the bovine vimentin-encoding cDNA. Gene **140:** 257–259
67 Hofmann I., Herrmann H. and Franke W. W. (1991) Assembly and structure of calcium-induced thick vimentin filaments. Eur. J. Cell Biol. **56:** 328–341
68 Steinmetz M. O., Stoffler D., Hoenger A., Bremer A. and Aebi U. (1997) Actin: from cell biology to atomic detail. J. Struct. Biol. **119:** 295–320
69 Chrétien D., Metoz F., Verde F., Karsenti E. and Wade R. H. (1992) Lattice defects in microtubules: protofilament numbers vary within individual microtubules. J. Cell Biol. **117:** 1031–1040
70 Nicholl I. D. and Quinlan R. A. (1994) Chaperone activity of α-crystallins modulates intermediate filament assembly. EMBO J. **13:** 945–953
71 Imoto T. (1997) Stabilization of protein. Cell. Mol. Life Sci. **53:** 215–223
72 Winter H., Langbein L., Praetzel S., Jacobs M., Rogers M. A., Leigh I. M. et al. (1998) A novel human type II cytokeratin, K6hf, specifically expressed in the companion layer of the hair follicle. J. Invest. Dermatol. **111:** 955–962
73 McGowan K. and Coulombe P. A. (1998) The wound repair-associated keratins 6, 16, and 17: insights into the role of intermediate filaments in specifying keratinocyte cytoarchitecture. In: Intermediate Filaments: Subcellular Biochemistry, vol. 31, pp. 173–204, Herrmann H. and Harris J. R. (eds.), Plenum, New York
74 Porter R. M., Hutcheson A. M., Rugg E. L., Quinlan R. A. and Lane B. E. (1998) cDNA cloning, expression, and assembly characteristics of mouse keratin 16. J. Biol. Chem. **273:** 32265–32272
75 Capetanaki Y. and Milner D. J. (1998) Desmin cytoskeleton in muscle integrity and function. In: Intermediate Filaments: Subcellular Biochemistry, vol. 31, pp. 463–495, Herrmann H. and Harris J. R. (eds.), Plenum, New York
76 Stumptner C., Zatloukal K., Magin T. M., Fuchsbichler A., Franke W. W., Baribault H. et al. (1998) Pronounced liver pathology in aged keratin 8 and keratin 18 knockout mice. Mol. Biol. Cell 9: 165a, Abstract 957
77 Ku N.-O., Michie S. A., Soetikno R. M., Resurreccion E. Z., Broome R. L. and Omary M. B. (1998) Mutation of a major keratin phosphorylation site predisposes to hepatotoxic injury in transgenic mice. J. Cell Biol. **143:** 1–10